전력전자학술대회 논문집 2004. 7.12 ~ 7.15

능동 클램프 풀브릿지 부스트 컨버터에 대한 모델링 및 분석

金 萬 高
부 경 대 학 교

Modeling and Analysis of Active-Clamp, Full-Bridge Boost Converter

Marn-Go Kim
Pukyong National University

ABSTRACT - Recently, an active-clamp, full-bridge boost converter has been actively studied for high-power applications such as power factor correction and battery discharger. However, DC and AC modeling for this converter has not conquered.

In this paper, a DC and small-signal AC modeling for the active-clamp, full-bridge boost converter is described. Based on the operation principle, the ac part of the converter can be replaced by a dc counterpart. Then, a conceptual equivalent circuit is derived by rearranging the switches. The equivalent circuit for this converter consists of CCM (Continuous conduction mode) boost and DCM (Discontinuous conduction mode) buck converter. The analyses for the equivalent CCM boost and DCM buck converter are done using the model of PWM switch. The theoretical modeling results are confirmed through experiment or SIMPLIS simulation.

1. Introduction

Active clamp circuits have been widely used for absorbing inductive energy and reducing overshoot voltage across semiconductor switching devices. As a result, considerable improvements have been made in several converter topologies using active clamp [1]-[4].

Recently, a novel high-power bidirectional dc/dc converter has been proposed for fuel-cell powered electric vehicles[5]-[6]. The power can flow in either direction. One direction of power flow is the conventional voltage-fed phase-shift full-bridge converter. This operation is described in [3]. The other direction of power flow is an isolated active-clamp, full-bridge boost converter. The active-clamp, boost converter can be used for various high-power applications such as power-factor correction and battery discharger.

To design feedback compensator, small-signal modeling for a converter is needed. In this paper, a dc and small-signal modeling for the active-clamp, full-bridge DC/DC converter is performed. Based on the operation principle, the ac part of the converter can be replaced by a dc counterpart. Then, a conceptual equivalent circuit is derived by rearranging the switches. The equivalent circuit for this converter is represented as continuous conduction mode(CCM) boost converter followed by discontinuous conduction mode(DCM) buck converter. The analyses for the equivalent CCM boost and DCM buck converter are done using the model of PWM switch[7]-[8]. The modeling results are confirmed through experiment or simulation.

2. Modeling of Active-Clamp, Full-Bridge Boost Converter

The switching pairs in diagonal positions are operating at duty cycles larger than 0.5. The boost inductor is charged during the period when all the four switches are on, and discharged when one diagognal switch pair is off and the clamp switch is on. The operational modes and typical waveforms are shown in Fig. 2.

Mode I: All the bridge switches are on and the clamp switch is off. The transformer leakage current is zero. The boost inductor is charged as in the conventional boost converter.

Mode II: One diagonal switch pair S3-S4 is off and the clamp switch is on. Vpn is charged up to the clamp capacitor voltage, and then the transformer leakage current is ramped up linearly by the voltage difference between the clamp capacitor and the reflected output voltage. In the steady state, the discharging current from the clamp capacitor is equal to charging current. Because the discharging clamp capacitor current can flow through the transformer current, the peak transformer current is higher than the input inductor current.

Mode III: Sc is turned off, and suddenly makes the transformer leakage current higher than the input inductor current. The surplus current discharges the parasitic switch capacitance between p and n. When Vpn goes down to zero, the switch pair S3-S4 is turned on, resulting in zero voltage switching. The transformer leakage current is reset

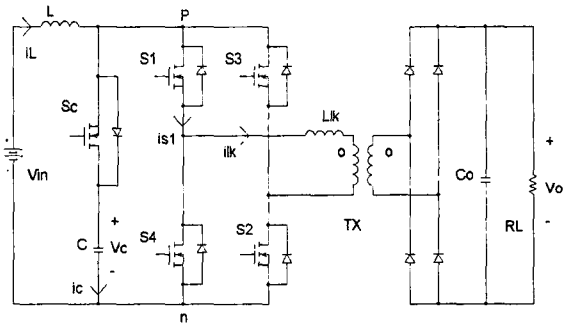

Fig. 1 Active-clamp, full-bridge boost converter

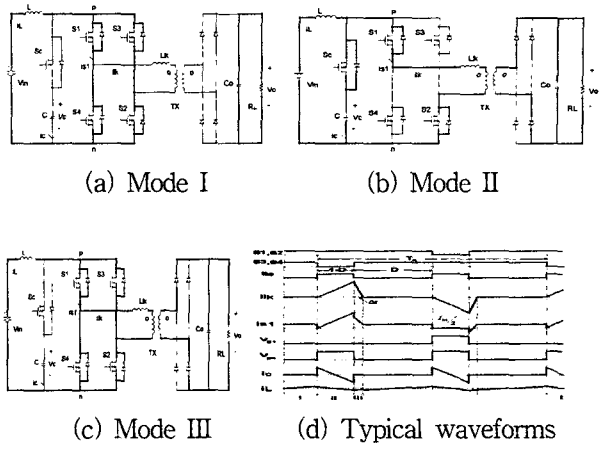

(a) Mode I (b) Mode II

(c) Mode III (d) Typical waveforms

Fig. 2 Operational modes and typical waveforms

to zero. After this mode, the next half cycle of operation is initiated.

To perform dc and small-signal analysis for the active-clamp full-bridge converter, understandable conceptual equivalent circuit is derived in Fig. 3. In the original circuit, 4 full-bridge switches transform DC signal into AC signal, the AC signal is transferred into secondary part of the transformer through leakage inductor, and then the bridge diodes rectify the AC signal to make the output voltage. The original circuit has a difficulty to be analyzed mainly due to the AC part that can not be averaged. If the AC part of the original circuit is replaced by a DC counterpart, a DC equivalent circuit can be obtained. In the DC equivalent circuit, S_ and Sc are operated in a complementary switching function to S. Mode I is during the interval when S is on and the primary-side diode is off. Mode II is when S is off and the diode is on. Mode III is when S is on and the diode is on. If the switch configuration of Fig. 3(b) is transposed without any change of switching function between any two points of A, B, and C, the conceptual equivalent circuit can be derived. The conceptual equivalent circuit is represented as the continuous conduction mode (CCM) boost and the discontinuous conduction mode (DCM) buck converter.

Fig. 4. shows simulated state waveforms to compare between original and conceptual equivalent

circuits operating under the same input and output conditions. Basically, the magnitudes of the state waveforms for the conceptual equivalent circuit are equal to those of the original circuit. The only difference between the two circuits is that the leakage current in conceptual equivalent circuit is DC while the leakage current in the original circuit is AC.

The conceptual equivalent circuit is the combination of well-known two topologies, CCM boost and DCM buck. Now, we can go ahead to analyze the original circuit. The PWM switches can be designated as three terminals which consists of active, passive, and common respectively (refer to a1, p1 and c1 for CCM boost, and a2, p2 and c2 for DCM buck shown in Fig. 5). The PWM switch model represents the dc and small-signal characteristics of the nonlinear part of the converter. Using the PWM switch model [7]-[8], DC and small-signal models for Fig. 4(c) are shown in Fig. 5. and Fig. 6, respectively.

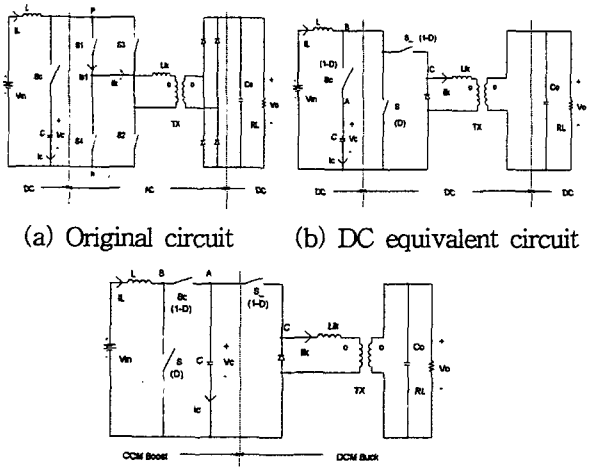

(a) Original circuit (b) DC equivalent circuit

(c) Conceptual equivalent circuit

Fig. 3 Derivation of conceptual equivalent circuit

3. Analysis

To perform small-signal analysis, DC operating points are determined. In this paper, the PWM switch models from [7]-[8] are substituted in the

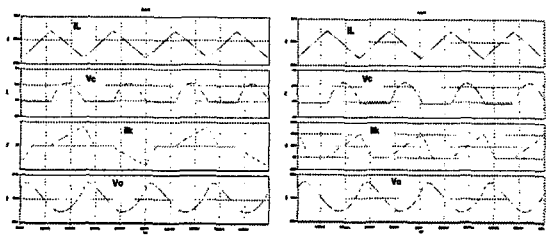

(a) Original (b) Conceptual

Fig. 4 Comparison of simulated state waveforms between original and conceptual equivalent circuits

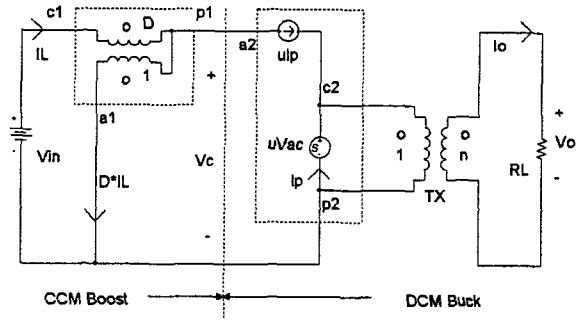

Fig. 5 DC model

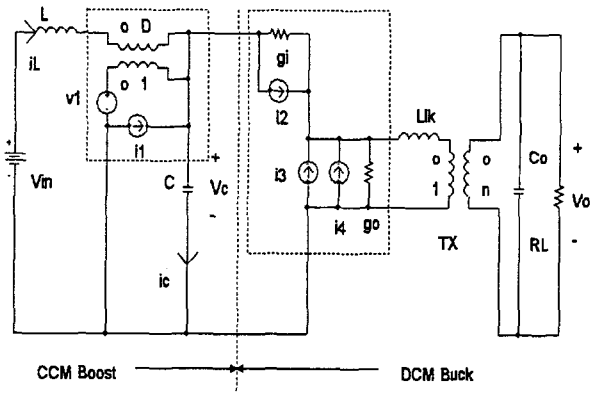

Fig. 6 Small-signal AC model

CCM boost and DCM buck conveters as shown in Fig. 5 and Fig. 6. Note that the output voltage of this DCM buck converter is controlled by (1-d) while that of the DCM buck converter in [8] is controlled by d. As a result, D and $\hat{d}$ of the PWM switch model in [8] for DCM buck converter are changed to 1-D and $-\hat{d}$ for this DCM buck

converter, respectively.

The DC operating point parameters are determined as :

$M_1 = V_c / V_{in} = 1/(1-D)$, $I_L = I_o \cdot M$

where M = Vo / V_{in} .

$$u = \frac{(1-D)^2}{K \cdot M_2} \quad , \quad K = \frac{2L_{lk} \cdot F_s}{R_L / n^2} \quad ,$$

$$F_s = 2/T_s$$

$$M_2 = V_{c2p2}/V_c = \frac{2}{1+\sqrt{1+4K/(1-D)^2}}$$

DC voltage gain M = Vo / V_{in} = $M_1 \cdot M_2 \cdot n$

$$V_{a2c2} = V_{ac} = V_c - V_o/n$$

$$V_{c2p2} = V_o/n$$

$$I_{c1} = I_{a1} + I_{p1} \ , \ I_{c2} = I_{a2} + I_{p2}$$

$$I_{c1} = -I_L \ , \ I_{p1} = -I_{a2} = -D' \cdot I_L$$

$$I_{a1} = -D \cdot I_L \ , \ I_{c2} = n \cdot I_o$$

$$I_{p2} = I_p = n \cdot I_o - D' \cdot I_L$$

Next, we can evaluate the small-signal parapeters at the dc operating point as follows :

$$v_1 = \frac{V_{a1p1}}{D}\hat{d} = -\frac{V_c}{D}\hat{d}$$

$$i_1 = I_{c1}\hat{d} = -I_L\hat{d}$$

$$g_i = \frac{I_{a2}}{V_{a2c2}} = \frac{D' \cdot I_L}{V_c - V_o/n}$$

$$i_2 = -\frac{2 \cdot I_{a2}}{1-D}\hat{d} = -\frac{2 \cdot D'I_L}{1-D}\hat{d}$$

$$i_3 = \frac{2I_{p2}}{V_{a2c2}}\hat{v}_{a2c2} = \frac{2(nI_o - D'I_L)}{V_c - V_o/n}\hat{v}_{a2c2}$$

$$i_4 = -\frac{2I_{p2}}{1-D}\hat{d} = -\frac{2(nI_o - D'I_L)}{1-D}\hat{d}$$

$$g_o = \frac{I_{p2}}{V_{c2p2}} = \frac{(nI_o - D'I_L)}{V_o/n}$$

To perform DC and small-signal analyses, the following circuit parameters are used :

L = 1 μH, C = 58 μF, L_{lk} = 0.1 μH, C_o = 0.68 μF, R_L = 72 Ω, V_{in} = 24 V, V_o = 600 V, T_s = 10 μs, F_s = 200 *kHz* , transformer turns ratio n = 18.

Assuming n=1, the normalized DC voltage gain

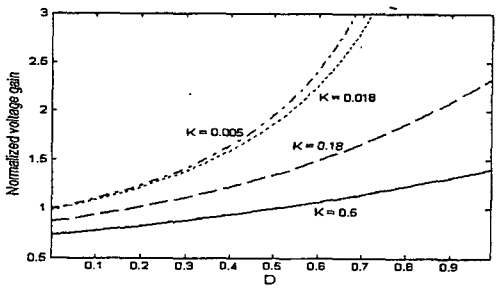

Fig. 7 Normalized DC voltage gain as a function of D and K

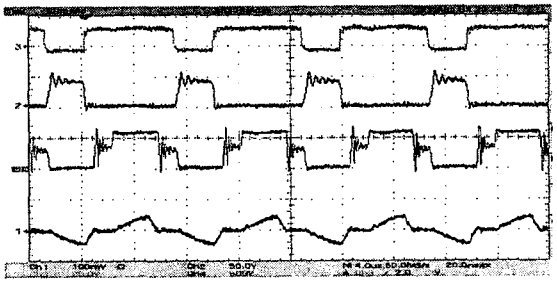

(a) Vin = 24 V, time scale: 4 μs/div, Upper to lower traces : Vg3 [20 V/div], Vds3 [50 V/div], output diode Vd1 [500 V/div], i_{lk}/n [50 A/div]

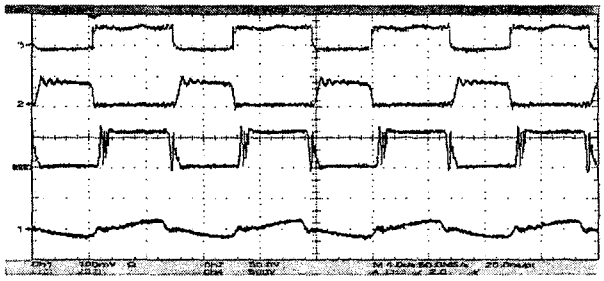

(b) Vin = 30 V, time scale: 4 μs/div, Upper to lower traces : Vg3 [20 V/div], Vds3 [50 V/div], output diode Vd1 [500 V/div], i_{lk}/n [50 A/div]

Fig. 8 Experimental waveforms at different input voltages

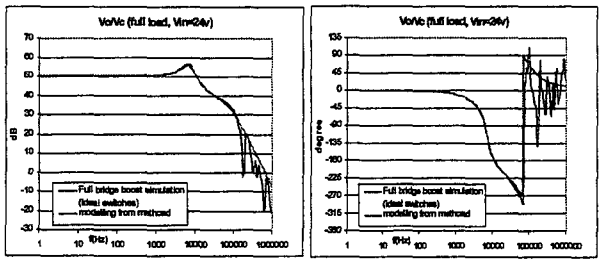

Fig. 9 Control input-to-output voltage transfer function

curve for the active-clamp, full-bridge converter is plotted as a function of duty ratio D and K in Fig. 7. The DC voltage gain is increased as D is increased or K is reduced. Because K is inversely proportional to the load resistance, the DC voltage gain is increased at the light load. From this figure, we can determine the range of duty ratio for given load and voltage gain ranges.

Fig. 8 show the duty ratio change according to the different input voltages of 24 V and 30 V at 5 kW output power. To obtain the output voltage of 600 V with n = 18 , the normalized voltage gains are 1.389 for 24 V and 1.11 for 30 V. When the output power is 5 kW, the load resistance value is 72 Ω and the parameter K is 0.18. With the normalized voltage gains and K, the duty ratios from Fig. 7 become 0.53 for 24 V and 0.3 for 30 V , respectively. Note that the secondary leakage inductor current i_{lk}/n is increasing during (1-d). The experimental waveforms show good agreement with theoretical results.

The small-signal control-to-output transfer function for the converter at the above operating point are plotted and compared with the results of SIMPLIS simulation as shown in Fig. 9, respectively. The conceptual equivalent circuit modeling presented in this paper show good agreement with the simulation results.

4. Conclusion

The DC and small-signal modeling for the active-clamp, full-bridge converter is performed. To achieve the modeling, the original circuit is transformed into the conceptual equivalent circuit, which consists of CCM boost and DCM buck. Substituting the PWM switch models into the PWM switches of the conceptual equivalent circuit, the DC and small-signal modeling can be accomplished.

Using the derived modeling, static and dynamic characteristics for the converter are analyzed. Normalized DC voltage gain curve is presented as a function of D and K. The normalized voltage gain is proportional to D, but inversely proportional to K.

The control-to-output transfer function for the converter is plotted. The small-signal characteristic for the converter shows fourth-order system. This small-signal modeling can be extended to design the feedback compensators. The theoretical modeling results are confirmed through experiment or simulation.

This work was supported by Pukyong National University Research Abroad Fund in 2002.

References

[1] C. S. Leu, G. Hua and F.C. Lee, " Comparison of the Forward Circuit Topologies with Various Reset Schemes, " in Proceedings of VPEC Seminar, 1991 , pp. 101-109.

[2] J.A. Sabate, V. Vlatkovic, R.B. Ridley and F.C. Lee, "High-Voltage, High-Power, ZVS, Full-Bridge PWM Converter Employing An Active Snubber, " in Proceedings of the APEC, 1991, pp. 158-163.

[3] J.G. Cho, G.H. Rim and F.C. Lee, " Zero Voltage Current and Zero Current Switching Full Bridge PWM Converter Using Secondary Active Clamp, " in Proceedings of the PESC, 1996, pp. 657-663.

[4] R. Watson and F.C. Lee, " A soft-switched, full-bridge boost converter employing an active- clamp circuit, " in Proceedings of the PESC, 1996.

[5] K. Wang, F.C. Lee, and J. Lai, " Bi-Directional Full-Bridge DC/DC Converter with Soft-Switching Scheme , Part I: Principles of Operation, " in Proceedings of VPEC Seminar, 1998 , pp. 143-149.

[6] K. Wang, L. Zhu, D. Qu , H. Odendaal, J. Lai, and F.C. Lee, " Bi-Directional Full-Bridge DC/DC Converter with Soft-Switching Scheme , Part II: Design, Implementation, and Experimental Results, " in Proceedings of VPEC Seminar, 1998.

[7] V. Vorperian, " Simplified Analysis of PWM Converters Using the Model of the PWM Switch, Part I: Continuous Conduction Mode, " in Proceedings of VPEC Seminar, 1989 , pp. 1-9.

[8] V. Vorperian, " Simplified Analysis of PWM Converters Using the Model of the PWM Switch, Part II: Discontinuous Conduction Mode, " in Proceedings of VPEC Seminar, 1989 , pp. 10-20.